Paving the way for the use of reinforced thermoplastic pipes for the transport of carbon dioxide

Sjoerd Jansma
Kiwa Technology
the Netherlands

Peter Cloos
SoluForce
the Netherlands

Summary
This paper describes the high-pressure carbon dioxide permeation testing of a reinforced thermoplastic pipe and the chemical resistance to carbon dioxide of the piping materials. A permeation model was used to determine the partial carbon dioxide pressure that each material is subjected to.

Keywords
Reinforced thermoplastic pipe (RTP), carbon dioxide (CO_2), permeation, chemical resistance

Abstract
One of the few ways that energy-intensive industries can substantially reduce their carbon dioxide (CO_2) emissions in the short term is Carbon Capture, Utilisation, and Storage (CCUS). This technology will require a CO_2 transport system between the carbon capture site and the storage site. This provides an opportunity for new piping systems. However, changing the transported medium to CO_2 means that the properties of the medium will change. This affects the product performance, which needs to be reconsidered and defined accordingly. This paper describes the tests and model used to define the behaviour of a reinforced thermoplastic pipe (RTP), specifically its chemical resistance and susceptibility to permeation of carbon dioxide.

The resistance to carbonic acid (a product of CO_2 and water) of the gas-tight layer was determined by using the permeation model to define the conditions in combination with information from literature.

The resistance to rapid gas decompression (RGD) of a high-density polyethylene (HDPE) liner was demonstrated by submerging test pieces in supercritical CO_2 at 156 bar and 65 °C and rapidly reducing the pressure to atmospheric conditions for 20 cycles. The test identified no formation of blisters, slitting or other defects.

The permeation rate of the RTP was determined by carrying out a full-scale permeation test of the product at 40 bar and 65 °C using gaseous CO_2.

The results presented in this paper show that RTPs are a mature product and can compete with steel pipes for the transport of carbon dioxide at high pressure and temperature, making them an excellent alternative piping system for CCUS.

Introduction
The RTP system under consideration has been used for several decades [1, 2], primarily in the oil and gas industry. Current developments present an opportunity to use the RTP system for CCUS applications. However, as the application is new, the product performance when used to transport CO_2 is unknown. Using RTPs to transport CO_2 requires reconsideration and determination of the properties of the product when exposed to CO_2, including the resistance to permeation and chemical resistance of the product.

Theoretical background

RTP

The studied spoolable reinforced thermoplastic pipe is a multilayer pipe produced by SoluForce and coded as M570 GT (see figure 1). From the inside out, the pipe consists of the following elements (or layers):

1) Fluid-tight, corrosion-resistant HDPE liner
2) Aluminium gas-tight layer
3) Synthetic fibre reinforcement for strength
4) White HDPE cover to protect against UV, abrasion and solar heating

The product is suitable for use at temperatures of up to 65 °C and gas operating pressures of up to 40 bar(g) (even though the LCL is 90 bar).

Figure 1. Overview of the studied spoolable reinforced thermoplastic pipe.

Permeation

This section considers the theoretical background and formulas for the permeation of gaseous CO_2, although these formulas can be adapted to describe liquid CO_2 or even supercritical CO_2.

Permeation is a naturally occurring process in which the permeate (in this case CO_2) passes through a solid barrier material (the various elements of the RTP). We can consider the permeation process as a flow of the permeate through a material, expressed as the permeation rate (Q). The material acts as a resistance (R) that impedes the permeation process. The driving force of the whole process is the difference in concentration (C). This can be expressed as:

$$C = Q \times R \tag{1}$$

The permeation rate depends on the variables in equation (1):

- The driving force: the difference in the concentration of the permeate on each side of the barrier. For an ideal gas, the concentration of the permeate can be expressed as the partial pressure (p_{gas}). In equation (1), c can be replaced by p.
- The resistance: this depends on the dimensions of the barrier, both the layer thickness (e) and the surface area (A), and the natural conductivity of the permeate through the material, expressed as the permeability coefficient (P_C). For polymeric materials, this is calculated as:

  $$R = \frac{e}{P_C \cdot A} \tag{2}$$

  It is important to define the geometric shape of the barrier and the route the permeate takes as it passes through each element. The area of the geometric shape often changes as the permeate passes through. Consider, for instance, a cylindrical homogenous pipe: the area on the inside is smaller than the area on the outside of the pipe. This can be resolved in three ways, given in order of increasing accuracy [3]:
  - By defining the best ‘average’ value for the area. For the example, this can be achieved by deriving the area from the median diameter.

- By subdividing the element into smaller elements and combining the resistances of each element. For the example, this can be achieved by dividing the cylindrical pipe into several thinner cylindrical pipes. The thinner cylinders can be slid together to form the original cylindrical pipe.
- By integration of the geometric shape. For the example, this can be achieved by using the thinner cylindrical pipes from the previous step and making the wall thickness of each pipe as small as possible. This can be achieved using a limit where the increment reaches zero, which can be converted to an integral.

Temperature also has a major effect on permeation, as it affects the mobility of molecules and polymers, which in turn affects the natural conductivity of the material as expressed in terms of the permeability coefficient. The permeability coefficient thus increases with temperature [4]. The permeation test in this paper was performed at a single temperature: the maximum operating temperature. This resulted in a worst-case permeation rate for the RTP.

Chemical compatibility

The product in this study has been used for several decades [1, 2] to transport media including oil and gas. This track record, along with extensive product knowledge, provides a sound foundation for this study. The benchmark product properties are therefore known and do not need to be defined. What does need to be defined, is whether and how CO_2 can affect these properties. Based on the properties of CO_2, we defined the areas of focus for this study. For instance, CO_2 is relatively inert and unlikely to have a direct chemical interaction with the HDPE liner. This was confirmed by various literature sources [5, 6, 7]. A verification of the chemical compatibility of the HDPE liner was therefore sufficient, and extensive studies to determine the chemical reactivity were deemed unnecessary.

In contrast, CO_2 is known to be a powerful solvent. CO_2 may therefore affect the physical compatibility of the HDPE liner. However, HDPE was found to be compatible with CO_2 [5, 6, 7] and there is no indication that PE dissolves in CO_2, even at 270 °C and 1750 bar [8]. This allows us to be confident that the liner material is suitable for use with CO_2. However, for this specific application, a rapid gas decompression (RGD) event could affect the product. During such an event, the dissolved CO_2 can increase in volume due to the loss of pressure. This could result in blistering, crack formation or tearing [9]. Tests were performed to determine if RGD could result in material failure of the liner.

The resistance of the aluminium gas-tight layer to water was also studied. The impurities present in the CO_2 mixture depend on the CO_2 production and handling processes [10, 11]. Some impurities may also enter the CO_2 due to permeation from the environment through the pipe. As the presence and number of impurities vary with the application, it is difficult to cover them all in this paper. One exception was however made, namely the potential presence of water as an impurity. CO_2 can react with water to form carbonic acid. In contrast to CO_2, carbonic acid has acidic properties, which could affect the compatibility of the material. HDPE is known to have excellent resistance to acids. Metals, however, may corrode.

The precise effects of CO_2 on each RTP element depend on the conditions. The most prominent are the four thermodynamically stable phases of CO_2, which are all within the range of common RTP operating conditions (based on temperature and pressure). The phases are:

1) gaseous CO_2 (gCO_2)
2) liquid CO_2 (lCO_2)
3) compressible liquid CO_2 (cCO_2)
4) supercritical CO_2 (sCO_2)

The phases significantly change the behaviour of CO_2 and as such need to be accounted for. The conditions that each element is exposed to are affected not just by the operating

conditions, but also largely by the product performance. The liner and the gas-tight layer shield the reinforcement layer and cover from the effects of the transported medium. As such, the pressure of the CO_2 at the outside of the product is far lower than at the inside. The liner and gas-tight layer may therefore be exposed to sCO_2 or cCO_2, while the shielded reinforcement layer and cover are exposed to gCO_2. A permeation model was used to determine the level of shielding. This analysis confirmed the above example. In addition to the permeation model, a full-scale permeation measurement was carried out. This information was subsequently used to determine the material compatibility for use with CO_2.

This permeation model also helps to answer hypothetical questions, including one considered in this paper: “If a pinhole where to be present in the gas-tight layer, how would it affect the permeation behaviour of the product?”

Method

Permeation model: permeation through a multilayer pipe

To define the permeation rate of a multiplayer pipe, the individual elements need to be combined to form a single description of the flow of the permeate. This can be achieved by determining the resistance of each element and combining these resistances based on their respective position, in a manner similar to that employed in the fields of electricity and thermodynamics:

- In series: $$p_{gas} = Q_p \cdot (R_1 + R_2) \quad (3)$$
- In parallel: $$p_{gas} = Q_p \cdot \left(\frac{1}{\frac{1}{R_1} + \frac{1}{R_2}} \right) \quad (4)$$

The reasoning is explained in [12]. The resistance of each element is determined by defining the geometric shape of the element, the route the permeate follows as it passes through the element and the permeability coefficient found in literature or experimentally derived.

Once the resistances of all the elements are known, the total flow of permeate (Q) can be calculated. The permeation rate of the product and the resistance of each individual element are then used to calculate the permeation rate through that element. In a series arrangement, the flow of permeate is equal for all the elements. In a parallel arrangement, the flow is divided across the individual elements in proportion to their resistances. Once Q is known for each element, the driving force (expressed as the partial CO_2 pressure (p_{CO2})) for that specific element can be derived using equation (1).

Full-scale permeation

Jacket pipes were installed around each pipe section as shown in figure 2. A CO_2 sensor (*ATU-21 from Atal*) was placed inside each jacket pipe to measure the accumulation of the permeated CO_2. The CO_2 sensor was validated prior to testing using reference gases with known CO_2 concentrations in a climate chamber at 85 °C. The CO_2 concentration inside the jacket pipe was also verified using gas chromatography at a single point in time. The entire setup was placed inside a climate chamber at 65 °C.

The piping system was subsequently flushed with pure CO_2 and pressurised to 40 bar(g). Both the leak tightness of the jacket pipes and the RTP were checked using pressure measurements.

The CO_2 concentration, temperature and pressure were monitored over time. Because the internal volume of the jacket pipes and the external volume of the components inside the jacket pipe were known, the annular volume was also known. The annular volume was used to convert the CO_2 concentration to the CO_2 quantity. If the upper limit of the CO_2 sensor was reached, the jacket pipe was flushed with nitrogen gas.

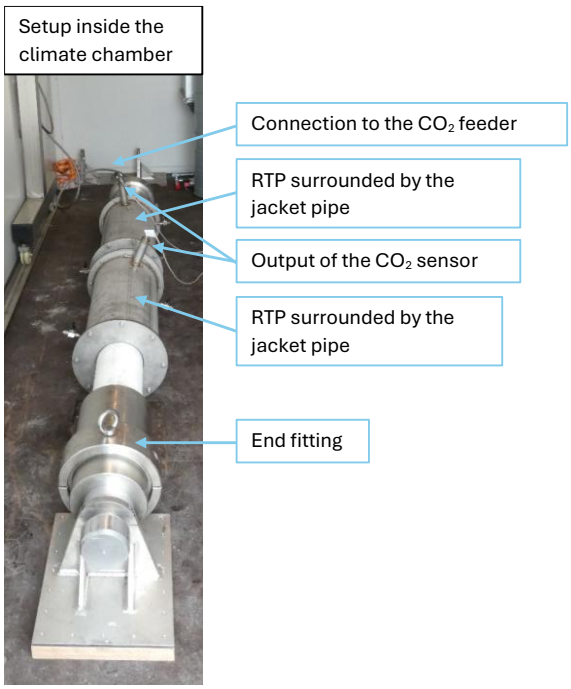

Figure 2. Overview of the test setup for the piping system.

Following an initial phase without any permeation (the time lag), accumulation inside the metal jacket pipe began after several days. After somewhat more time, a stationary permeation phase was reached in which a linear increase in concentration occurred over time. The permeation rate (in [ml(STP)] CO_2 per [day] at 40 [bar(g)]) was calculated from the slope of this part of the curve. The permeation rate for the RTP was corrected to take account of the length of the pipe segments and the measured pressure.

Rapid gas decompression

The test method was implemented in accordance with both ISO 13628-2 and API 17J:2017. Six test bars of the liner material were prepared from the spoolable reinforced thermoplastic pipe segment. They were 140 mm in length, 20 mm wide and 6 mm thick. The test bars were placed inside a container pressurised with CO_2 at 156 bar and 65 °C. The temperature and pressure were both monitored throughout the test. The system was left for 2 weeks to ensure that the saturation level exceeded 95%. The system was then depressurised at a rate exceeding 70 bar/min. A total of 20 pressurisation and depressurisation cycles were conducted. After each pressurisation, the samples were left for over 23 hours to stabilise. Following these cycles, the test bars were visually examined using optical microscopy (20x magnification). Cross sections of the test bars were also visually examined. Contrary to the test procedure described in ISO 13628-2 but in line with § 6.2.3.3 of API 17J, the test bars were visually examined after the completion of all 20 cycles rather than after each individual cycle.

As the liner test bars were immersed in sCO_2 at 156 bar and 65 °C for over 6 weeks (2 weeks saturation, 4 weeks of RGD cycles), the test bars could also provide information about other solvent-related effects. The mass and dimensions were therefore measured before and after immersion. Information about the chemical composition of the material was also obtained by generating a pyrogram (using gas chromatography with a flame ionisation detector (Py-GC/FID)) and comparing this to the pyrogram of an unexposed reference. This resulted in the pyro-index. These tests were carried out at least 20 days after extraction to allow any absorbed CO_2 to deplete.

Result

Permeation model

The permeation model in the most basic form for the RTP is given below. The contribution of each element to the total resistance of the permeation is calculated using equation (2) and expressed as a percentage:

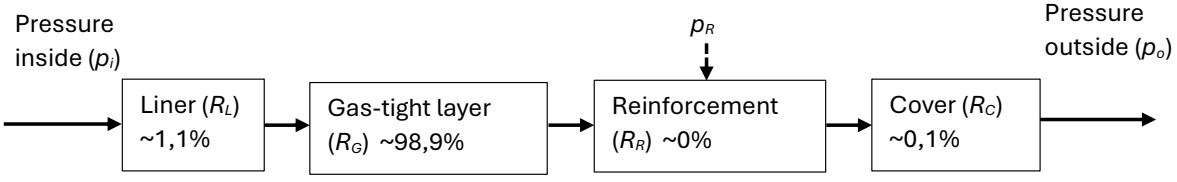

This model assumes the resistance of the reinforcement layer to be zero, as the reinforcement is non-bonded.

By rewriting equation (1) by replacing *C* with the pressure difference (p_i - p_o) and including equation (3), the model is expressed as:

$$Q_p = \frac{(p_i - p_o)}{R_L + R_G + R_R + R_C} \quad (4)$$

The partial CO_2 pressure at the inner side of the reinforcement layer (p_R) can be calculated using:

$$p_R = p_i - R_L \cdot Q_P - R_G \cdot Q_P = p_o + R_C \cdot Q_P \quad (5)$$

As equation (4) can be substituted into equation (5), the partial CO_2 pressure between each element can be derived using the calculated resistances and the inside and outside CO_2 pressure. This was carried out for the reinforcement layer (p_R), which resulted in a value of less than 0,1% of the operating pressure (p_i). This shows that the liner and gas-tight layer shield the reinforcement layer and cover. As such, the chemical compatibility of the reinforcement layer and cover must account for 0,1% of the operating pressure.

Depending on the topic under consideration, one can extend the model by considering additional elements. If a circular pinhole with a diameter of 1 mm were present in the gas-tight layer in each metre of pipe, it would change the permeability of the product. This would result in the following permeation model. The resistance of each element is again calculated using equation (2):

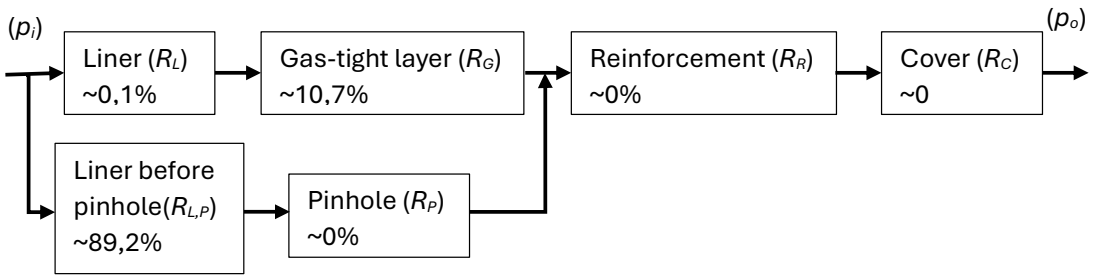

Which can be expressed as:

$$Q_p = \frac{(p_i - p_o)}{\left(\frac{1}{\frac{1}{R_L + R_G} + \frac{1}{R_{L,P} + R_P}} + R_R + R_C\right)} \quad (6)$$

This model is based on several assumptions. As the resistance of the reinforcement layer is expected to be zero, it is expected that the individual parallel flows will come together in this layer to form a single flow through the cover.
Secondly, the resistance of the pinhole in the gas-tight layer is expected to be zero.
Finally, the permeate must first pass through a section of the liner before it travels through the pinhole. The chosen shape of the liner section is based on a hemisphere. The base of the hemisphere covers the pinhole and has a diameter of twice the wall thickness plus the diameter of the pinhole. This is based on the following consecutive assumptions:

- The liner just in front of the pinhole has a substantial influence on the overall permeability, as it has a limited free volume, which restricts the permeate passing through the pinhole.
- The permeate will follow the path of least resistance. If the distance that the permeate travels through the liner is greater than the layer thickness of the liner, the permeate will pass directly from the transported medium rather than following this diversion. The hemisphere is therefore limited by the layer thickness of the liner.

By comparing equations (5) and (6) with the resistances provided in the permeation model, it was determined that a pinhole with a diameter of 1 mm in each metre of pipe will result in an increase in the permeation rate of the RTP of approximately 12%.

Chemical compatibility

Aluminium is compatible with CO_2: one well-known existing application is the use of aluminium gas cylinders to store pressurised CO_2. This method has been used for several decades for beer [13]. Other sources confirm the suitability of aluminium for use with humid CO_2 under a variety of conditions, including temperatures of up to 400 °C and pressures of up to 40 bar [13].

However, if aluminium comes into direct contact with water saturated with CO_2, the acidity as result of the formation of carbonic acid may become too severe. The acidity is mostly affected by the CO_2 pressure, as shown in table 1. The difference in pH between 1,13 bar at 23 °C and 6 bar at 95 °C is negligible, while the pH is far lower for 154 bar at 35 °C. For this RTP, the aluminium that is exposed to the transported medium is protected by the HDPE liner, which prevents direct contact with water. The permeation model also shows that the conditions affecting the aluminium in contact with the environment are far less severe, as the CO_2 pressure on that side is only 0,1% of the operating pressure. The acidity on this side is therefore limited to a pH of ~3,7. Although literature sources indicate that the aluminium layer should be able to withstand this low pH, due to carbonic acid, this still has to be confirmed experimentally.

Table 1. Acidity of water fully saturated with CO_2 under the given conditions.

Temperature [°C]	Pressure [bar]	Acidity of the water [pH]
23	1,13	3,7 [9]
35	154	2,97 [14]
95	6	3,97 [15]

Full-scale permeation

The accumulated CO_2 volume in the jacket pipes for the first 23 days is presented in figure 3. The first 10 days show typical permeation behaviour. It takes time for the CO_2 to break through the pipe wall before it accumulates in the metal jacket pipe: in this case, approximately 6 days. After 6 days, the permeation rate starts to stabilise. As the upper limit of the CO_2 sensors was reached after 11 days, the jacket pipes were flushed on day 19.

The jacket was flushed 13 times in total (not all shown in the graph). The highest five consecutive permeation rates resulted in an average of 270 ml/(m·day), corrected for the length of the pipe segment and the measured pressure. This corresponds to 0,5 g/(m·day). The lowest corresponding coefficient of determination (R^2) of the slopes is 0,997, which is found favourably high (very close to the maximum 1, indicating a perfect correlation). The temperature during testing was 65 ± 2 °C.

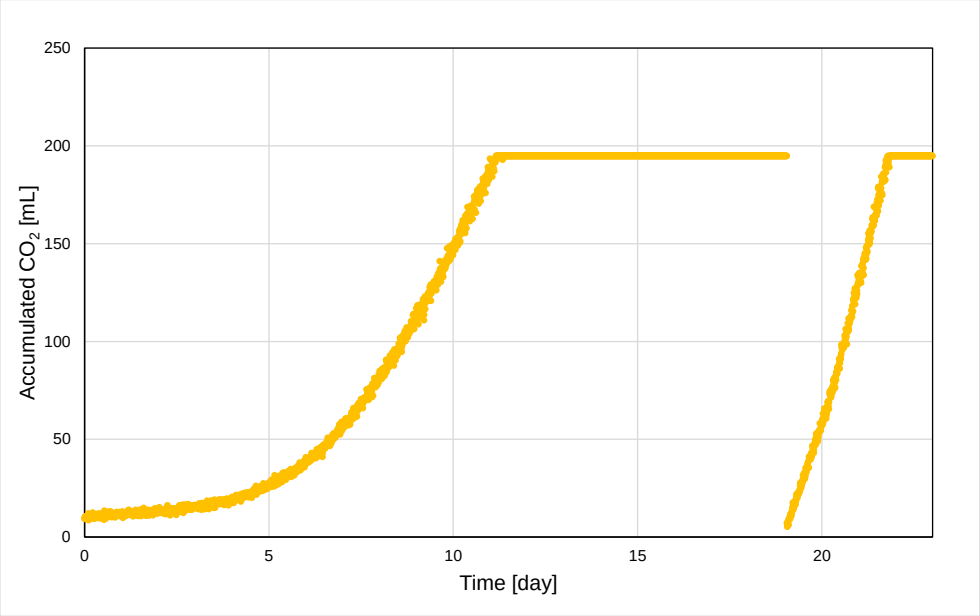

Figure 3. The accumulated CO_2 in the jacket pipes over time.

Rapid gas decompression

After careful examination of both the outside and cross section of the test bars, no signs of blisters, slitting or other defects could be observed. As an example, the cross section and inner pipe wall of a test bar at 20x magnification are given in figure 4. The PE liner material meets the requirements of ISO 13628-2 and API 17J:2017.

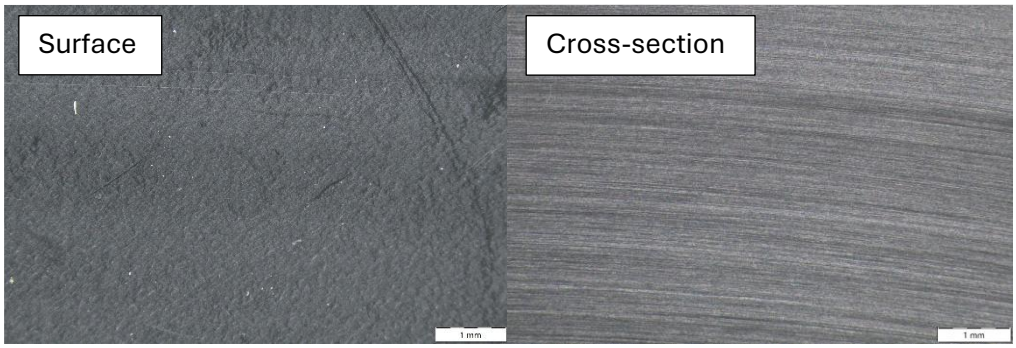

Figure 4. Visual examination of a test bar, both the surface and the cross-section, after 20 RGD cycles starting at 156 bar and 65 °C. No blisters or slitting can be observed.

The average and standard deviation of the dimensions and mass of test bars before and after immersion are given in table 2. No statistically significant differences were observed (using a paired t-test with a confidence interval of 95%). The analysis software calculated a pyro-index of 0,992, which means no significant differences in material composition are present.

Table 2. Dimensions and mass of the test bars before and after exposure to 156 bar CO_2 at 65 °C.

		Thickness [mm]	Width [mm]	Length [mm]	Mass [g]
Before	Average	6,06	20,53	145	16,51
	Standard deviation	0,37	0,46	0,0	1,04
After	Average	6,10	20,48	145	16,47
	Standard deviation	0,37	0,49	0,1	1,04
Difference	Average	+0,04	-0,05	0	-0,04

Discussion

Rapid gas decompression

The soaking time of 2 weeks was sufficient to reach 95% saturation in the liner material, because in the full-scale permeation test a steady state permeation began after six days at constant temperature. Compared to the RGD, this is a slower process as:

- The CO_2 feed in the full-scale test is from one side (the inside of the pipe), whereas the feed in the RGD is from all sides (as the test bars are immersed).
- During the full-scale test, the CO_2 must pass through all the elements before it accumulates in the metal jacket pipe. The results therefore also include the soaking of the gas-tight layer, reinforcement layer and cover.

This test demonstrated the compatibility of the HDPE liner with rapid gas decompression events. However, the permeation model showed that the inside of the gas-tight layer is also exposed to high partial CO_2 pressures. It is therefore also necessary to study the RGD resistance of the gas-tight layer for future work.

No significant changes were observed in the PE liner material after six weeks of exposure to sCO_2 at 156 bar and 65 °C by studying the mass, dimensions and material composition (pyrolysis). Since other literature sources also confirm the compatibility of HDPE with CO_2, the PE liner was deemed to be compatible. However, a slight difference was observed in the pyrogram. This may be due to the loss of an additive from the liner, which remains below detection limits. Our expert opinion is that this will not affect the performance of the pipe.

Permeation comparison

Just as the pressure and temperature range, the permeation rate of CO_2 is a description of the performance of the tested RTP. Whether it meets the requirements depends on the criteria, which depend on specific circumstances. At this point, no relevant criteria for the CO_2 emissions of an RTP are known to us, which means these cannot be used as a reference. In the absence of this information, we compared the permeation value with another reference, in this case a car.

The Toyota Corolla (the second best-selling car model in 2024, with 1,08 million units sold [16]) in the hatchback Icon 1.8 hybrid configuration (lowest CO_2 emissions in this model range) has CO_2 emissions of 102 g/km (worldwide harmonised light vehicle test procedure) [17]. The RTP emits 0,5 g/(m·day) due to permeation. The annual CO_2 emissions of one kilometre of RTP at 40 bar and 65 °C due to permeation therefore equal the CO_2 emissions of one Toyota Corolla traveling 1800 km, which corresponds to the distance of the Dutch border to Warsaw in Poland and back again.

Conclusion

Carbon dioxide permeation

A permeation model was developed for the RTP. This model was used to design a chemical compatibility study of the RTP by determining the partial CO_2 pressure of each element in the pipe. The model was also used to determine the effects of specific alterations, including a pinhole in the gas-tight layer.

The permeation of CO_2 through the RTP was measured. The highest five consecutive permeation rates resulted in an average of 270 ml/(m·day) at 40 bar CO_2 and 65 °C.

Chemical compatibility

We found no indications that the materials in the tested RTP are unsuitable for transporting CO_2. This paper focuses on the chemical compatibility of:

- the solvent interactions between CO_2 and the liner material, particularly the resistance to rapid gas decompression.

- the carbonic acid degradation of the gas-tight layer.

Using literature references, material experiments and the permeation model, both effects were found to not affect the RTP in a significant way.

References

[1] M. Wolters, W. Wessing, L. Dalmolen, R. Eckert and J. Wuest, “Reinforced thermoplastic pipeline (RTP) systems for gas distribution,” *23rd World Gas Conference, IGU, Amsterdam,* 2006.

[2] D. v. Ameln and W. Wessing, “Aramid-reinforced plastic pipes, High-strength pipes for gas transport,” *Proceedings of the International Gas Research Conference, Vancouver,* 2004.

[3] E. v. d. Stok, F. Scholten and L. Dalmolen, “Cover blow-off resistance of reinforced thermoplastic pipes for gas service,” *Plastic Pipes XV Conference - Vancouver, BC Canada, September 20-22,* 2010.

[4] B. Flaconnèche, J. Martin and M. Klopffer, “Permeability, Diffusion and Solubility of Gases in Polyethylene, Polyamide 11 and Poly(vinylidene fluoride),” *Oil & Gas Science and Technology,* vol. 56, no. 3, p. 261.278, 2001.

[5] ISO 23936-1:2022, “Petroleum, petrochemical and natural gas industries - Non-metallic materials in contact with media related to oil and gas production - Part 1: Thermoplastics”.

[6] ISO/TR 10358:2021, “Plastics pipes and fittings for industrial applications - Collection of data on combined chemical-resistance”.

[7] Plastics Pipe Institute, “Chemical resistanc of plastic piping materials - TR-19:2020,” 2020.

[8] S. Paul, R. Shepherd and P. Woollin, “Selection of materials for high pressure CO2 transport,” *Paper presented at Third International Forum on the Transportation of CO2 by Pipeline,* 2012.

[9] AMI, “Supercritical Carbon Dioxide in the Oil and Gas Industry (presentation),” *Oil and Gas Non-Metallics - London, UK, December 7-8,* 2022.

[10] K. Johnsen, H. Holt, K. Helle and O. K. Sollie, “Mapping of potential HSE issues related to large-scale capture, transport and storage of CO2,” *DNV,* 2009.

[11] C. Okezue and D. Kuvshinov, “A comprehensive study of the effect of chemical impurities on selection and sizing of centrifugal machines for supercritical carbon dioxide transport pipelines,” *Applied Energy,* vol. 230, pp. 816-835, 2018.

[12] S. Jansma, P. Cloos and E. v. d. Stok, “Testing spoolable reinforced flexible pipes and liner material for high-pressure hydrogen transport,” *Plastic Pipes XX Conference - Amsterdam, the Netherlands, September 6-8,* 2020.

[13] C. Vargel, “Corrosion of Aluminium,” *Elsevier (ISBN: 0 08 044495 4),* 2004.

[14] C. Peng, J. P. Crawshaw, G. C. Maitland, J. M. Trusler and D. Vega-Maza, “The pH of CO2-saturated water at temperatures between 308 K and 423 K at pressures up to 15 MPa.,” *The journal of supercritical fluids,* vol. 82, pp. 129-137, 2013.

[15] L. Ansaloni, B. Alcock and T. A. Peters, “Effects of CO2 on polymeric materials in the CO2 transport chain: A review,” *Greenhous Gas Control,* vol. 94, 2020.

[16] Statista, “Best-selling passenger car worldwide in 2024,” 2025. [Online]. Available: https://www.statista.com/statistics/239229/most-sold-car-models-worldwide.

[17] Toyota, “Toyota Corolla Technical Specification - Ref:210713M,” *obtained from media.toyota.co.uk.*

